 Cytometry 45:102–114 (2001)

Validation of Flow Cytometric Competitive Binding Protocols and Characterization of Fluorescently Labeled Ligands

Anna Waller,[1] David Pipkorn,[1] Karyn L. Sutton,[1] Jennifer J. Linderman,[1] and Geneva M. Omann[2*]

[1]Department of Chemical Engineering, University of Michigan, Ann Arbor, Michigan
[2]Departments of Biological Chemistry and Surgery, University of Michigan Medical School and Veteran's Administration Medical Center, Ann Arbor, Michigan

Received 19 December 2000; Revision Received 6 July 2001; Accepted 15 July 2001

Background: Fluorescently labeled ligands and flow cytometric methods allow quantification of receptor-ligand binding. Such methods require calibration of the fluorescence of bound ligands. Moreover, binding of unlabeled ligands can be calculated based on their abilities to compete with a labeled ligand. In this study, calibration parameters were determined for six fluorescently labeled N-formyl peptides that bind to receptors on neutrophils. Two of these ligands were then used to develop and validate competitive binding protocols for determining binding constants of unlabeled ligands.

Methods: Spectrofluorometric and flow cytometric methods for converting relative flow cytometric intensities to number of bound ligand/cell were extended to include peptides labeled with fluorescein, Bodipy, and tetramethylrhodamine. The validity of flow cytometric competitive binding protocols was tested using two ligands with different fluorescent properties that allowed determination of rate constants both directly and competitively for one ligand, CHO-NLFNYK-tetramethylrhodamine.

Results: Calibration parameters were determined for six fluorescently-labeled N-formyl peptides. Equilibrium dissociation constants for these ligands varied over two orders of magnitude and depended upon the peptide sequence and the molecular structure of the fluorescent tag. Kinetic rate constants for CHO-NLFNYK-tetramethylrhodamine determined directly or in competition with CHO-NLFNYK-fluorescein were statistically identical.

Conclusions: Combination of spectrofluorometric and flow cytometric methods allows convenient calculation of calibration parameters for a series of fluorescent ligands that bind to the same receptor site. Competitive binding protocols have been independently validated. Cytometry 45:102–114, 2001. © 2001 Wiley-Liss, Inc.

Key terms: neutrophils; fluorescence calibration; binding kinetics; G-protein coupled receptor; N-formyl peptide receptor; flow cytometry

The relationship between receptor-ligand binding and processing and cellular responses may be elucidated, at least in part, by determining values of the rate constants for receptor/ligand binding and processing (1,2,3). One can ask, for example, whether the initial rate of ligand binding correlates with the timing of the cellular response, or if there are other rate-limiting steps involved. Are the rates of receptor desensitization ligand-dependent, and does this contribute to differences in ligand efficacy? The answers to these and related questions require a quantitative method for obtaining rate constants for receptor-ligand binding and processing with a variety of ligands.

Receptor-ligand binding can be monitored by spectrofluorometry or flow cytometry when a fluorescently labeled ligand is available. Compared to radioligand methods, flow cytometry offers the advantage of monitoring ligand binding to single cells in real time without the need to separate bound from unbound ligands. These binding data can be collected on a microsecond time scale and, because single-cell fluorescence is measured, the heterogeneity in the binding properties of the population of cells can be detected. The background fluorescence of the unbound ligands is minimized by the small volume probed by the flow cytometric laser, on the order of the volume of a single cell.

However, this is only the case for high-affinity ligands. For a low-affinity ligand (i.e., large equilibrium dissociation constant, K_d), a higher ligand concentration is required to reach the same number of bound receptors as a

Grant sponsor: National Science Foundation; Grant number: BES-9713856. Grant sponsors: Office of Research and Development, Medical Research Service, Department of Veteran's Affairs; the Alfred P. Sloan Foundation, and the GE Foundation.

*Correspondence to: Geneva M. Omann, Research Service (11R), Veteran's Administration Medical Center, 2215 Fuller Road, Ann Arbor, MI 48105
E-mail: gmomann@umich.edu-

high-affinity ligand, thus there is more free ligand present in the media. This free ligand contributes to the apparent background fluorescence and can lead to the inability to distinguish bound versus unbound ligand. Thus competitive protocols have been developed in which binding of an unlabeled ligand is calculated based on its ability to influence the binding of a fluorescent ligand. A goal of this work is to validate these competitive binding protocols.

Because flow cytometry measurements give fluorescence on a relative intensity scale, one can only convert fluorescence readings to numbers of bound ligands if an appropriate calibration technique is available. Fay et al. (4) have reported methods for calibrating fluorescein-labeled ligands to free fluorescein and for evaluating possible quenching of fluorescein-labeled ligand upon binding to the receptor. An additional goal of this paper was to expand upon the calibration methods of Fay et al. (4) to include ligands labeled with fluorophores other than fluorescein. We report calibration values for the fluorescently labeled ligands N-formyl-norleucyl-leucyl-phenylalanyl-phenylalanyl-lysine-fluorescein (CHO-NLFFK-FL), N-formyl-norleucyl-leucyl-phenylalanyl-norleucyl-tyrosyl-lysine-Bodipy (CHO-NLFNYK-Bodipy), and N-formyl-norleucyl-leucyl-phenylalanyl-norleucyl-tyrosyl-lysine-tetramethylrhodamine (CHO-NLFNYK-TMR), all of which bind to the N-formyl peptide receptor on human neutrophils. In addition, we confirm the values reported by Fay et al. (4) for N-formyl-methionyl-leucyl-phenylalanyl-lysine-fluorescein (CHO-MLFK-FL), N-formyl-methionyl-leucyl-phenylalanyl-phenylalanyl-lysine-fluorescein (CHO-MLFFK-FL), and N-formyl-norleucyl-leucyl-phenylalanyl-norleucyl-tyrosyl-lysine-fluorescein (CHO-NLFNYK-FL). These calibration methods are applicable to any cell surface receptor system for which a fluorescently labeled ligand can be obtained, given the constraints of flow cytometric sensitivity and ligand affinity as discussed by Murphy (5). We also report equilibrium binding constants for various N-formyl peptides and estimates of their quenching caused by interaction with the receptor.

We then used two of these ligands to validate the competitive binding protocols. Flow cytometry requires the attachment of a fluorescent tag to the ligand, which could lead to the inability of the ligand to bind with the receptor or elicit a cellular response. To monitor the binding of unlabeled ligands, or native ligands, competitive binding methods have been used (6–8). Given information on the binding of the fluorescent ligand alone, the binding of the unlabeled ligand can then be calculated indirectly from its affect on the binding of labeled ligand. This approach is attractive because many unlabeled ligands are available and they can be used without regard to K_d because distinction of bound and free unlabeled ligands is not an issue. Although competitive binding has been used to calculate binding rate constants for unlabeled ligands, this technique has never been independently verified.

Utilizing two labeled ligands with different fluorescence characteristics, we now report the independent validation of competitive binding protocols for accurately determining the rate constants for a two site receptor system, the N-formyl peptide receptor system on the human neutrophil.

The N-formyl peptide receptor on the neutrophil is capable of binding to many short peptide sequences (9–11), including fluorescently labeled peptides, and elicits responses that include chemotaxis, oxidant production, and phagocytosis. Pioneering work by Sklar et al. (12) and more recently by Hoffman et al. (8) have demonstrated that the binding of several N-formyl peptides, CHO-NLFNYK-FL, N-formyl-norleucyl-leucyl-phenylalanyl (CHO-NLF), and N-formyl-methionyl-leucyl-phenylalanyl (CHO-MLF), at 4°C can be described by the two site receptor binding scheme:

$$L + R_s \underset{k_r}{\overset{k_f}{\rightleftharpoons}} LR_s \xrightarrow{k_x} LR_x \underset{k_{f2}}{\overset{k_{r2}}{\rightleftharpoons}} L + R_x \qquad \text{(Model I)}$$

Ligand (L) binds to surface receptors (R_s) with rate constant k_f to form low-affinity receptor-ligand complexes (LR_s), which convert to high-affinity complexes (LR_x) with rate constant k_x. High-affinity complexes are also formed by ligand binding to high-affinity state receptors (R_x) with the rate constant k_{f2}. Ligand can dissociate from low- or high-affinity receptor-ligand complexes with rate constants k_r and k_{r2}, respectively. At 4°C, receptor trafficking is minimized and the total number of surface receptors, R_{tot}, equal to the sum of the receptor states described above, remains constant. Because the low-affinity receptor/ligand complex is believed to be the receptor state responsible for signaling (8,13) the rate constants, k_f, k_r, and k_x, which govern the formation and lifetime of the low-affinity receptor-ligand complex, may be critical for determining cellular response characteristics.

The two hexapeptides, CHO-NLFNYK-FL and CHO-NLFNYK-TMR, were utilized for validating the competitive binding protocol by evaluating independently the kinetic binding rate constants that describe the interaction between these ligands and the N-formyl peptide receptor. These direct measurements were then compared with values of kinetic binding rate constants evaluated via a competitive binding protocol in which CHO-NLFNYK-FL was the "labeled" ligand and CHO-NLFNYK-TMR the "unlabeled" ligand. The similarity of CHO-NLFNYK-TMR rate constants determined by direct and competitive protocols validates the competitive protocols.

MATERIALS AND METHODS

Reagents

Standard cellular and ligand buffer (HSB) contained 5 mM KCl, 147 mM NaCl, 1.9 mM KH_2PO_4, 0.22 mM Na_2HPO_4, 5.5 mM glucose, 0.3 mM $MgSO_4$, 1 mM $MgCl_2$, and 10 mM HEPES, at pH 7.4. To minimize loss of peptide ligand caused by nonspecific binding to containers, 1 mg/ml (0.1%) bovine serum albumin was added to HSB. Bovine serum albumin (BSA), tert-butyloxycarbonyl-phenylalanyl-leucyl-phenylalanyl-leucyl-phenylalanine (t-Boc), N-formyl-methionyl-leucyl-phenylalanine (CHO-MLF), triethylamine, and fluorescein were obtained from Sigma-

Aldrich Chemical Co. (St. Louis, MO). CHO-NLFNYK-FL, CHO-NLFNYK-Bodipy, and CHO-NLFNYK-TMR were obtained from Molecular Probes, Inc. (Eugene, OR) and CHO-MLFK-FL from Peninsula Laboratories, Inc. (Belmont, CA). All ligands were stored in stock solutions of 10^{-3} M in dimethylsulfoxide (DMSO; Pierce Chemical Co., Rockford, IL). Other solvents, chloroform, methanol (MeOH), and acetic acid were obtained from Fisher Scientific (Chicago, IL).

Synthesis and Purification of Fluorescein-Labeled Pentapeptides

The pentapeptides CHO-MLFFK and CHO-NLFFK were synthesized by the Peptide Synthesis Facility of the University of Michigan. Each peptide was reacted with fluorescein isothiocyanate (Molecular Probes, Inc., Eugene, OR) (14,15). The fluorescein-labeled peptides were purified from the reaction mixture on tapered silica gel plates (Uniplate-T taper plates from Analtech, Newark, DE) using chloroform/MeOH/triethylamine (5/3/1) as described by Sklar (14). The labeled peptide bands were scraped and eluted in MeOH. Quantification of the recovered material was achieved by measuring the absorbency at 495 nm of product in MeOH on a Gilford spectrophotometer using an extinction coefficient of 8.1×10^4 for FITC labeled peptide (16). After quantification of the product, the MeOH was evaporated and the product dissolved in DMSO and stored at −20°C. Purity of the ligands was confirmed by HPLC analysis and thin layer chromatography. HPLC was performed with a Vydac C-18 column using a gradient solvent system. Solvent A was 99.9% water and 0.1% trifluoroacetic acid, and solvent B was 19.9% water, 80% acetonitrile, and 0.1% trifluoroacetic acid. The gradient of solvent B was run from 0 to 100% in 40 min at 0.7 mL/min. Thin layer chromatography on silica gel G and GF (2.5 × 7.5 cm plates) was performed with two solvent systems: chloroform/MeOH/triethylamine (5/3/1; v/v/v) and chloroform/methanol/acetic acid (3/1/0.01; v/v/v) (14,17).

Neutrophil Isolation

Neutrophils were isolated via the protocol of Tolley et al. (18) and maintained at 4°C in HSB buffer at 10^8 cell/ml until used for experiments (within 2 h of isolation).

Calibration of Fluorescently Labeled Ligand

Spectrofluorometric determination of F. Emissions from solutions of free fluorescein and fluorescently labeled ligands were measured on a spectrofluorometer (SLM-Aminco 8100, Urbana, IL) to calculate the quantum yield ratio F much as described by Fay et al. (4). The ratio F is the number of free ligands per fluorescein equivalent (the ratio of the quantum yield of fluorescein to that of free ligand). The emission wavelength used for the fluorescein- and Bodipy-labeled ligands was 530 nm and for the tetramethylrhodamine labeled ligand was 580 nm. These correspond closely to the wavelengths of the flow cytometer detectors, FL1 and FL2 (see below).

Free fluorescein was dissolved in nanopure water to a final concentration of 10^{-3} M and then diluted 1:100 in HSB/BSA. Further dilutions into spectrofluorometer cuvettes (Fisher Scientific, Pittsburgh, PA) using HSB/BSA were made to give a concentration series with the range of 0.25×10^{-6} M to 1.50×10^{-6} M. The fluorescein concentrations were verified by absorbance measurements at 495 nm with the reported extinction coefficient of 7.25×10^4 (19).

Stock solutions of fluorescently labeled ligands, 10^{-3} M in DMSO in microcentrifuge tubes, were diluted to 10^{-5} M in DMSO. Serial dilutions of the fluorescently labeled ligands in the range of 0.25×10^{-6} M to 1.5×10^{-6} M in HSB/BSA were made in the spectrofluorometer cuvettes. The final concentration of the labeled ligand solutions contained 2.5–15% DMSO, which aided in the solubilization of the ligand; however, DMSO did not interfere with the absorbance and fluorescence measurements.[1] The concentrations of the fluorescein-labeled ligand were verified by absorbance measurements at 495 nm assuming an extinction coefficient of 8.1×10^{-4} for fluorescein-labeled peptide (16). The concentrations of the fluorescein-labeled ligands calculated from absorbance measurements corresponded to the concentrations based on the mass of ligand used for the dilutions. Hence for the nonfluorescein labeled ligands, the concentrations based on the mass of the ligand used were assumed to be correct.

Spectrofluorometric determination of quenching or enhancement of bound ligand fluorescence. The number of bound ligand molecules per fluorescein equivalent, Q, is crucial to quantifying kinetic binding data and is equal to the product of two ratios that can be determined independently:

$$Q = F \times I_b/I_f \quad (1)$$

where F is the number of free ligands per fluorescein equivalent (described above) and I_b/I_f is the ratio of fluorescence of bound ligand to free ligand (4). The fluorescence of a ligand can be enhanced or quenched upon binding to a receptor, and thus the value of I_b/I_f can be greater or less than one. Because antibodies that sufficiently quench the fluorescence of ligands labeled with Bodipy and tetramethylrhodamine were unavailable, the ratio of fluorescence of bound to free ligand, I_b/I_f, could not be quantitatively measured as has been done previously for fluorescein-labeled ligands (4). Quenching or enhancement of the fluorescently labeled ligand caused by interactions with the receptor was qualitatively evaluated by monitoring ligand binding on a spectrofluorometer. In stirred square cuvettes, the cellular background fluorescence of 1.5 ml of neutrophils at 10^7/ml in HSB/BSA was monitored for 20 s before a fluorescent ligand was added through a Hamilton syringe for a final concen-

[1] Varying the volume percentage of DMSO did not alter the fluorescence of free fluorescein; hence DMSO did not effectively alter the fluorescent moiety or solvent to effect the fluorescence of free fluorescein. In addition, the fluorescence of each fluorescein labeled ligand was the same when the volume percentage of DMSO was held constant at 10% as compared with when DMSO concentration varied from 2.5 to 15% (data not shown).

tration of 1 nM CHO-NLFFK-FL, 3 nM CHO-NLFNYK-Bodipy, and 5 nM CHO-NLFNYK-TMR. Ligands were either allowed to bind freely to the cell or blocked from binding by the presence of the N-formyl peptide receptor antagonist, t-Boc. t-Boc at 20 μM was allowed to prebind for about 1 min prior to the addition of the fluorescently labeled ligand.

The ligand concentrations utilized for these experiments were chosen to maximize the ratio of bound to free ligand with three experimental constraints in mind. First, a minimum of 1 nM ligand was required for its fluorescence to be reliably measured. Second, the maximum receptor concentration was limited by light scattering effects that became evident at high cell concentrations. A cell concentration of 10^7 cells/ml was the optimal concentration that would avoid these effects. Third, it was desirable to have a ligand concentration larger than the estimated equilibrium binding constant so that as many receptors as possible were bound, but low enough so significant free ligand depletion occurred.

Determination of Q with equilibrium binding analysis and flow cytometry. An alternative method for evaluating the calibration number Q (number of bound ligand molecules per fluorescein equivalent) relied on flow cytometric equilibrium binding data. These relative measurements can be converted to specific numbers of bound fluorescent ligand per cell (B) with the use of bead standards by;

$$B = M \times E \times Q \tag{2}$$

where M represents the flow cytometric measurement of mean channel per cell and E is the number of fluorescein equivalents per channel as calibrated by fluorescein-labeled bead standards. The quantum yield ratio (F from Eqn 1) for a well-characterized ligand that is not quenched upon binding, CHO-NLFNYK-FL, was used as a reference for evaluating the number of surface N-formyl peptide receptors, which were assumed constant for a particular cell preparation (4,20). The calibration values, Q, of the other fluorescently labeled ligands were then calculated. From these equilibrium-binding experiments, the equilibrium dissociation constants for the ligands were also evaluated. Predicted values of ligand quenching calculated with the use of Eqn 1 and F and Q values were compared qualitatively with spectrofluorometric quenching data.

The total number of N-formyl peptide receptors on the cell membrane was found using a 4°C equilibrium-binding assay described by Sklar and Finney (21). At 4°C receptor upregulation, internalization and recycling is minimized (3,8), and thus the total number of surface receptors can be assumed constant. In brief, a saturable binding curve was created by allowing various concentrations of a fluorescently labeled ligand to bind to cells for at least 1 h at 4°C in the dark. All concentrations were done in duplicate, and the specific concentrations were chosen in order to obtain binding data above and below the K_d. To account for nonspecific binding of the fluorescent ligand, some cells were blocked with a high concentration of an unlabeled ligand (10^{-5} M CHO-MLF) before the fluorescently labeled ligand was added. After at least 1 h of incubation, cells at 10^6/ml in HSB plus 1.5 mM Ca^{2+} were analyzed on a flow cytometer. The flow cytometer (Becton-Dickinson FACScan, San Jose, CA) was equipped with an argon laser with 488 nm excitation wavelength and two emission detectors: FL1, with a bandpass filter centered at 530 nm ± 30 nm, and FL2, with a bandpass filter centered at 585 nm ± 42 nm. For all measurements the compensation was set at zero. Incubation times longer than 1 h gave no significant difference in K_d or total number of surface receptors. The neutrophil population was gated based on the forward and side scatter light and the mean fluorescence intensity for each ligand concentration was calculated using CellQuest software (Becton-Dickinson, San Jose, CA).

Ligand fluorescence was calibrated daily to standard beads (Quantum 24, Flow Cytometry Standards Corp., Puerto Rico). These standard beads were labeled with fluorescein isothiocyanate (FITC) and the molecules of equivalent soluble fluorochrome (MESF) per bead, listed by the manufacturer, ranged from 3,000 to 65,000 MESF per bead. The reported fluorescein equivalents per standard bead were verified by comparison to standard fluorescein dilutions.

After subtraction of nonspecific binding from total binding, the concentrations of free ligands and specific receptor-ligand complexes were determined. The total number of surface N-formyl peptide receptors, R_{tot}, and the apparent equilibrium dissociation constant, K_{dapp}, were evaluated by minimizing the squared residual of the data points in a fit to a one site model (Eqn 3)

$$[LR] = \frac{R_{\text{tot}}[L]}{[L] + K_{d_{\text{app}}}} \tag{3}$$

where R_{tot} is the total number of surface receptors, [L] is the free ligand concentration and [RL] is the bound receptor concentration.

The calibration value Q for one fluorescently labeled ligand (CHO-NLFNYK-FL) was taken from the previously described spectrofluorometric calibration method. This value was used together with the standard beads in order to convert the mean fluorescence emitted to the number of bound ligands (Eqn 1). The R_{tot} for that particular experiment and K_{dapp} for the reference ligand were calculated from fitting the bound ligand data to the one-site model (Eqn 3). Once R_{tot} was established for that particular experiment, this value was kept constant while the calibration number Q and K_{dapp} were allowed to change when the equilibrium binding data for the other ligands were fitted to the one-site model. These equilibrium binding data of the reference ligand and the other test ligands were collected on the same day and with the same blood donor so that donor variability in the total number of surface receptors was not a factor. This analysis assumed that the reference ligand and the other ligands bound to the same site on the receptor. This was the case for N-formyl peptide ligands binding to the N-formyl peptide receptor as shown by competitive binding studies (7,9).

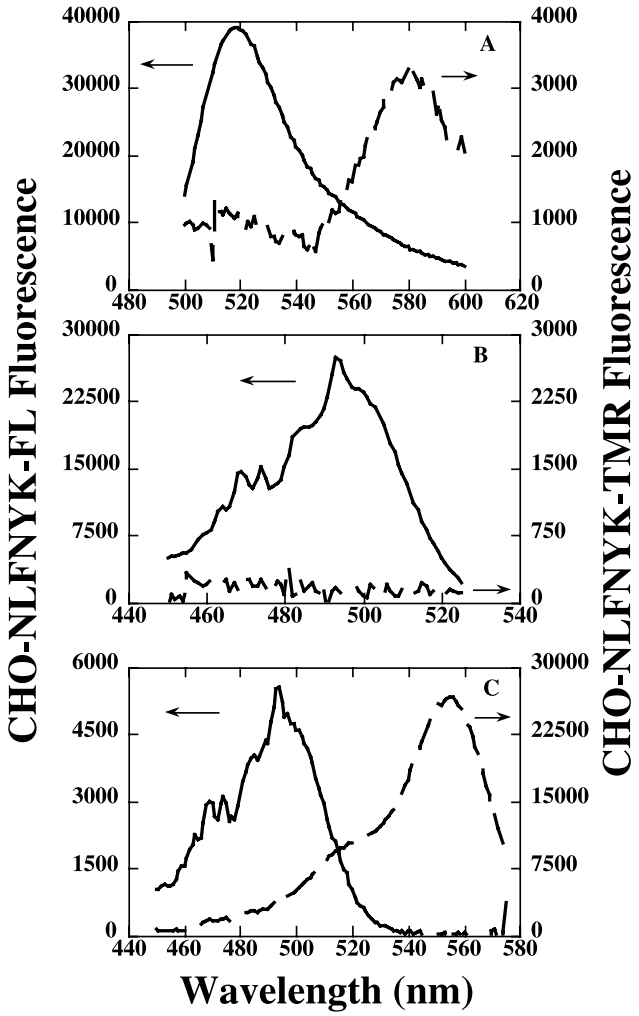

FIG. 1. Excitation and Emission spectra of CHO-NLFNYK-FL and CHO-NLFNYK-TMR. (**A**) Emission spectra monitored with 490 nm excitation on spectrofluorometer (SLM-Aminco 8100, Urbana, IL) from 100 nM ligand concentration in HSB with 1 mg/ml BSA. Excitation spectra monitored at 530 nm (**B**) and 580 nm (**C**). Specific emission or excitation shown in the figure was equal to the measured fluorescence minus the fluorescence of the carrier.

The same equilibrium binding protocol was utilized to evaluate total number of surface receptors (R_s) and equilibrium binding constant for labeled ligand (K_{dapp1}) for comparison with the competitive equilibrium binding protocol.

Validation of Competitive Binding Protocols

Choice of ligands for competitive binding protocol. When excited at a wavelength of 490 nm, CHO-NLFNYK-FL emits primarily at 520 nm while CHO-NLFNYK-TMR emission is detectable around 580 nm, as shown in Figure 1A. These emission wavelengths correspond with the emission wavelengths of FL1 and FL2 channels on the flow cytometer and therefore direct measurement of ligand binding was made using FL1 for CHO-NLFNYK-FL and FL2 for CHO-NLFNYK-TMR. Note that the broad spectrum for fluorescein was detectable at the higher wavelength (580 nm) and thus fluorescein-labeled standardized beads were also used for calibrating the FL2 signal. When equivalent concentrations of the two ligands were excited at a wavelength of 490 nm, the peak emission of the CHO-NLFNYK-TMR was approximately an order of magnitude less than that of the CHO-NLFNYK-FL (Fig. 1A), although this was still sufficiently intense to measure CHO-NLFNYK-TMR binding on FL2. The excitation spectrum for CHO-NLFNYK-FL peaks around 490 nm when emission is monitored at 530 nm, whereas the excitation spectrum peaks around 550 nm for CHO-NLFNYK-TMR when emission is monitored at 580 nm (Fig. 1B and C). In other words, although the detector filters of the particular flow cytometer utilized in this study was not optimal for the tetramethylrhodamine labeled ligand, the emission was detectable compared to background cellular fluorescence (see Fig. 2).

Equilibrium binding assay for labeled ligands. Equilibrium binding for labeled ligands was performed as described above for the determination of Q.

Kinetic binding assays for labeled ligands. For labeled ligands an association protocol (protocol A) and dissociation protocol (protocol B) were used and classified as "direct" kinetic binding measurements (8). Binding of CHO-NLFNYK-FL or CHO-NLFNYK-TMR was monitored on the flow cytometric detector centered at 530 nm (FL1) or 585 nm (FL2), respectively. The temperature was maintained at 4°C throughout the assay by keeping the cell samples in an ice-filled insulated beaker.

For protocol A, the autofluorescence of the unstimulated cells at 10^6 cells/ml in HSB plus Ca^{+2} was obtained

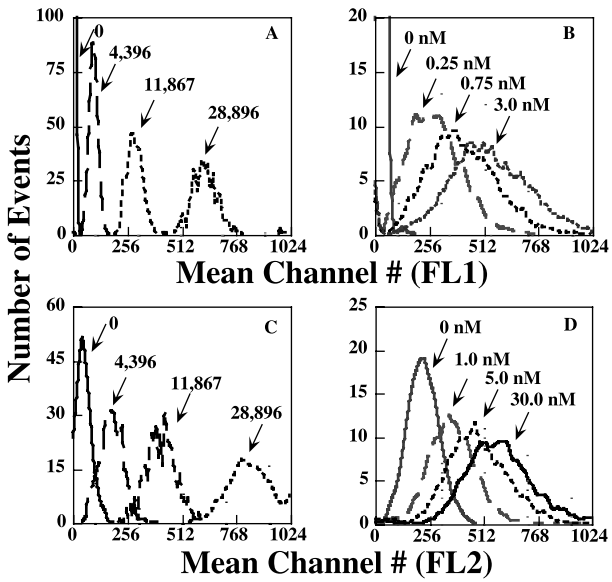

FIG. 2. Flow cytometric histrograms of beads and equilibrium binding samples. Equilibrium binding samples were prepared as described in Methods, and fluorescence was measured on the flow cytometer. Representative histograms at FL1, 530 nm emission, of the standard calibration FITC-labeled beads (**A**) and equilibrium binding of fluorescently labeled ligand CHO-NLFNYK-FL (**B**). Representative histograms at FL2, 585 nm emission, of the standard FITC-labeled calibration beads (**C**) and equilibrium binding of CHO-NLFNYK-TMR (**D**).

for about 7 s. At 10 s the fluorescently labeled ligand was added to the cell solution, and after quick mixing the tube was immediately returned to the flow cytometer for collection of data up to 3 min. It was crucial to minimize the time off-line after addition of the ligand, in our case approximately 3 s. The concentration of the ligand used was within an order of magnitude of K_{dapp}, as calculated from equilibrium binding data. Ligand and cell concentrations were chosen so that the free ligand concentration was not appreciably depleted by ligand binding (2) and the background fluorescence from the free ligand was minimized. Ligand concentrations of 3 nM and 6 nM for CHO-NLFNYK-FL and 15 nM and 30 nM for CHO-NLFNYK-TMR were used. Nonspecific binding was evaluated with cells preincubated with 3×10^{-5} M CHO-MLF before the addition of the labeled ligand.

For protocol B, neutrophils at 10^6 cells/ml in HSB plus Ca^{+2} were incubated with labeled ligands. At 90 s or 2 h, the binding of the labeled ligand was stopped by a rapid addition of an excess amount of a ligand blocker and the cell sample was quickly returned to the flow cytometer. The blocker CHO-MLF was added at a concentration at least a thousand fold higher than that of the labeled ligand, e.g., 3×10^{-5} M. The total time of data collection was 3 min. Dissociation was initiated after 90 s or 2 h of binding in order to capture different receptor affinity states.

Equilibrium binding assay for unlabeled ligand. As discussed and shown in Figure 1B, with 488 nm excitation and 530 nm emission (FL1) CHO-NLFNYK-FL appears as a labeled ligand and CHO-NLFNYK-TMR appears as an unlabeled ligand. Hence for the remaining discussion of the competitive binding protocols, CHO-NLFNYK-FL is referred to as the labeled ligand and CHO-NLFNYK-TMR is referred to as the unlabeled ligand. The equilibrium binding constant, K_{dappu}, for the unlabeled ligand was determined by competitive equilibrium binding (6,8). Mixtures of constant concentrations of the labeled ligand together with variable concentrations of the unlabeled ligand were allowed to bind to cells at 10^6/ml of HSB plus Ca^{2+} for at least 2 h at 4°C in the dark. Longer incubation times did not yield significantly different equilibrium dissociation constant estimates, and at least a 2-h incubation was determined sufficient for the ligand binding to reach equilibrium. Nonspecific binding was evaluated with cells preincubated with 3×10^{-5} M CHO-MLF before the mixture of labeled and unlabeled ligand was added. After equilibrium was reached the amount of bound labeled ligand was monitored on a flow cytometer and the specific bound data was fit to a single site binding model, where the labeled and unlabeled ligands were assumed to compete for the same receptor

$$\frac{[LR]}{R_{\text{tot}}} = \frac{[L]}{\frac{K_{d\text{app}_l}}{K_{d\text{app}_u}}([U] + K_{d\text{app}_u}) + [L]} \qquad (4)$$

where [U] is the concentration of the unlabeled ligand and K_{dappu} the equilibrium dissociation constant of the unlabeled ligand. The equilibrium dissociation constant for the labeled ligand, K_{dapp1}, was held constant at the value found in the previously described equilibrium binding assay.

Kinetic binding assays for unlabeled ligands. The binding of unlabeled ligand was evaluated by competitive binding of labeled and unlabeled ligand (8). Data were collected with the flow cytometric detector centered at 530 nm, and thus the "labeled" ligand was CHO-NLFNYK-FL and the "unlabeled" ligand was CHO-NLFNYK-TMR. The analogous measurements with the flow cytometric detector centered at 585 nm were not feasible because the broad spectrum of fluorescein was detectable at 585 nm, and much more intense than the tetramethylrhodamine emission. This low tetramethylrhodamine emission was because tetramethylrhodamine absorbance at 488 nm is about 5% that of absorbance at its maximum. Attempts to compensate for fluorescein fluorescence into the 585 nm channel resulted in unreliable data because of high background signal. Therefore competition by CHO-NLFNYK-FL while measuring CHO-NLFNYK-TMR was not evaluated. As with the direct kinetic binding assays, the competitive binding protocols (indirect kinetic binding assays) included an association protocol and a displacement protocol, and the temperature of 4°C was maintained through out the assay.

The competitive association protocol (protocol C) was the same as protocol A except that labeled and unlabeled ligands were added simultaneously. Concentrations of the unlabeled ligand and the labeled ligand were varied in order to optimize the measurements of labeled ligand binding and better distinguish the effect of the unlabeled ligand binding. With too much of the labeled ligand present, the effect of the competing unlabeled ligand was not detectable. Similarily, too much unlabeled ligand blocked the labeled ligand from binding, and the fluorescence measured was not distinguishable from nonspecific binding. Mixtures of 3 nM/15 nM, 6 nM/15 nM, and 6 nM/30 nM of CHO-NLFNYK-FL/CHO-NLFNYK-TMR, were utilized.

For the competitive displacement protocol (protocol D), unlabeled ligand (CHO-NLFNYK-TMR) was added initially and then displacement of unlabeled ligand was initiated by addition of labeled ligand (CHO-NLFNYK-FL). Hence there was an increase in fluorescence after displacement was initiated. For protocol D, cells at 10^6 cells/ml of HSB plus Ca^{+2} were allowed to bind with the unlabeled ligand until binding was interrupted by the rapid addition of the labeled ligand. For short-time displacement experiments, the unlabeled ligand was allowed to bind for 15–90 s prior to the addition of the labeled ligand, and the displacement of unlabeled ligand was monitored for approximately 3 min. Ligand concentrations used were 3 nM/15 nM and 6 nM/30 nM of CHO-NLFNYK-FL/CHO-NLFNYK-TMR. For long-time displacement experiments, the unlabeled ligand was allowed to bind for at least 15 min in order to convert the majority of the surface receptors to the high-affinity state. At this high-affinity state, the displacement of the unlabeled ligand by the labeled ligand was slow, and therefore the displacement of unlabeled ligand was monitored in incre-

ments of 2 min, for over 20 min. For the long-time displacement, the concentrations of the unlabeled and labeled ligands were optimized to quickly convert the receptors to the high-affinity state and to minimize the rebinding of unlabeled ligand after the addition of labeled ligand, hence the ligand concentrations were different from protocol C. The labeled ligand concentration was kept at least an order of magnitude larger than the concentration of the unlabeled ligand; 15 nM CHO-NLFNYK-TMR and 250 nM CHO-NLFNYK-FL were utilized. Another concern was the evaluation of the nonspecific binding caused by the high-labeled ligand concentration. Therefore a larger concentration of blocker was used in protocol D compared to all the other protocols. For the nonspecific binding, the cells were preincubated with 0.1 mM of the blocker, CHO-MLF, prior to the addition of the unlabeled and labeled ligand.

Analysis of kinetic binding data. Kinetic binding data were collected on the flow cytometer using Cell Quest Software (Becton Dickinson), which was used to gate the neutrophil population based on the forward and side scatter. The gated kinetic data was saved in Flow Cytometry Standard format (FCS) and moved to a UNIX platform, where the data was converted to ASCII. The data parameters, forward scatter, side scatter, and fluorescence, were averaged over each 200-ms time interval and the fluorescence values were converted to number of bound receptors by a specific ligand calibration value; 1.02 for CHO-NLFNYK-FL and 2.22 for CHO-NLFNYK-TMR (see previous sections). Nonspecific binding was described by a linear function and subtracted from the raw data yielding data of bound ligand per cell versus time. The total number of surface receptors, R_{tot}, and the equilibrium dissociation constant, K_{dapp}, were obtained from equilibrium binding analysis. Because of the irreversible conversion of the low-affinity state to the high-affinity state, K_{dapp} was assumed equal to the equilibrium dissociation constant, K_{dx}, for the high-affinity state of the receptor ($K_{dx} = k_{r2}/k_{f2}$) (8).

To determine the reaction rate constants for the labeled ligand, 2-h dissociation data from protocol B were analyzed first. After 2 h of binding, essentially all surface receptors were irreversibly converted to the high-affinity state. Hence the binding model could be reduced to a one-site binding model (8). The analytical solution for a one-site model was used to fit these data with the assumption that the free (unbound) labeled ligand concentration was zero after the addition of the blocker, CHO-MLF, which was present in great excess compared to the labeled ligand. The following equation was used in Microsoft Excel with the method of least squares to find the dissociation rate constant from the high-affinity receptor,

$$LR_x(t) = LR_{x,0}\exp(-k_{r2}t) \quad (5)$$

The value for the initial number of receptor-ligand complexes, $LR_{x,o}$, was obtained from averaging the number of high-affinity complexes from the first 10 s of data collection (before CHO-MLF is added). The value for k_{f2} was calculated from duplicates with the constraint of K_{dx}, and the average value of both k_{f2} and k_{r2} were held constant throughout the data analysis for that particular day.

Association data (protocol A) and 90-s dissociation data (protocol B) for labeled ligand were analyzed using equations describing the full two-site binding model (see Appendix) and the program Scientist (Micromath, Salt Lake City, UT), which utilized Powell's algorithm, a hybrid between the Gauss-Newton and steepest descent methods, to fit the data. The data were fit to minimize the sum of residuals with the assumption of constant absolute error and equal weight to all data points. Association data were fit by constraining the values of k_{f2} and k_{r2} as described above and allowing the values of k_f, k_r, and k_x to vary. Initial estimates were taken from Hoffman et al. (8). The criteria for further use of the evaluated rate constants was that the standard deviations of the fit values for the rate constants were at least an order of magnitude less than the rate constants themselves. The 90-s dissociation data from protocol B were analyzed with the assumption that the apparent labeled ligand concentration was zero after the addition of blocker. The blocker, CHO-MLF, was added at a concentration at least a thousand-fold greater than the labeled ligand concentration, which greatly reduced the probability of labeled ligand rebinding. Again, the parameters k_{r2} and k_{f2} were constrained as described above, while k_f, k_r, and k_x were allowed to vary. The values from association fits were used as initial guesses for their values. Analyses of both association and 90-s dissociation data yielded similar rate constants; however, 90-s dissociation data gave more confidence in k_x compared to the association data. The confidence was evaluated by the ratio of the rate constant estimate to standard deviation determined by Scientist for a particular fit. The reported average value for k_x includes values evaluated from both association and 90-s dissociation data.

Competitive binding data (both labeled and unlabeled ligands) were analyzed in the following way. Equilibrium binding data were analyzed using Eqn 4 to give K_{dappu}, assumed to be the dissociation constant for the high-affinity receptor state ($K_{du} = k_{r2u}/k_{f2u}$) for CHO-NLFNYK-TMR. The value of R_{tot} calculated from the competitive equilibrium data was consistent with the value calculated from direct equilibrium data. Kinetic binding data from protocols C and D were analyzed using Micromath Scientist and the equations in the Appendix to obtain rate constants for the unlabeled ligand. Rate constants for the labeled ligand (CHO-NLFNYK-FL) were held constant at the values determined by direct measurements described above. To make comparisons of the reaction rate constants evaluated by the different methods, direct and competitive, it was necessary to carry out both (i.e., protocols A–D) on the same day (same donor).

Analysis of long-time displacement data (protocol D) was done assuming that prior to the addition of labeled ligand, all receptors were in the high-affinity state and occupied by unlabeled ligand. This assumption was reasonable based on the time scale of data collection and estimated values of the initial binding rate constants, k_f, k_r, and k_x. Long-time displacement data were fit to two single-site binding models describing the binding of the labeled

Table 1
Summary of Calibration Values Evaluated Spectrofluorometrically, F, and Flow Cytometrically, Q, and Predicted Values for I_b/I_f Based on F and Q

Ligand	F[a,d]	Q[a]	I_b/I_f predicted[b]	F reported[c]	I_b/I_f reported[c]
CHO-NLFNYK-FL	1.02 ± 0.03 (3)	1.02 ± 0.00 (39)	1.00	1.26 ± 0.29	1.00
CHO-NLFNYK-Bodipy	2.60 ± 0.25 (4)	1.43 ± 0.07 (11)	0.55 ± 0.11		
CHO-NLFNYK-TMR	2.31 ± 0.32 (3)	2.22 ± 0.19 (30)	0.96 ± 0.31		
CHO-MLFFK-FL	2.13 ± 0.04 (2)	0.83 ± 0.07 (5)	0.39 ± 0.06	1.39 ± 0.51	0.54 ± 0.04
CHO-NLFFK-FL	2.14 ± 0.08 (2)	0.79 ± 0.06 (5)	0.37 ± 0.06		
CHO-MLFK-FL	0.92 ± 0.04 (4)	0.92 ± 0.06 (10)	0.99 ± 0.15	1.12 ± 0.13	0.72 ± 0.05

[a]Mean ± SEM, n in parentheses.
[b]Calculated from F and Q using Eqn 1.
[c]From Fay et al. (4) at 520 nm emission.
[d]Quantum yield ratio F calculated as described by Fay et al. (4) with the following arrangement: excitation monochromator set at 490 nm with slit widths of 2 nm and the excitation light filtered through a 10 nm bandpass filter centered at 490 nm (Corion, Holliston, MA). For fluorescein-labeled ligands, emission monochromator was set at 530 nm with slit widths of 1 nm, emitted light was additionally filtered with a 10 nm bandpass filter centered at 530 nm (Ealing, Holliston, MA), and an emission cut-off filter 3–70 (Kopp Glass, Inc., Pittsburgh, PA) was used to further reduce detection of scattered excitation light. For the tetramethylrhodamine labeled ligand, the emission monochromator was set at 580 nm with slit widths of 1 nm and emission light was further filtered using a 10 nm bandpass filter centered at 580 nm (Ealing, Holliston, MA). Emission was measured as 10 s of integrated photons.

and the unlabeled ligand to the high-affinity state of the receptor. The value of the reaction rate constant of k_{r2u} was evaluated using Scientist while holding the rate constants for the labeled ligand, k_{r2} and k_{f2}, constant and constraining k_{f2u} by K_{dxu}, as evaluated by the competitive equilibrium binding. After the duplicates of the long-time displacement data were analyzed, the reaction rate constants of k_{r2u} and k_{f2u} were averaged and held constant for that particular experiment.

Competitive association and short-time displacement data from protocols C and D were fit to the entire two-site binding model for both the labeled and the unlabeled ligand by Micromath Scientist. The data were analyzed under the constraints of reaction rate constants for the labeled ligand calculated earlier and the high-affinity reaction rate constants, k_{f2u} and k_{r2u}, from long-time displacement data, while k_{fu}, k_{ru}, and k_{xu} were allowed to vary. The assessment of a successful fit was the same as for the direct binding analysis.

The various reaction rate constants calculated from the direct and competitive binding assays were averaged per day (per donor), and the standard deviation caused by donor was also evaluated. The final reported values for the reaction rate constants are the averages of the daily averages, and the standard errors of the mean are based on the daily averages. The statistical analysis for comparison of the reaction rate constants for CHO-NLFNYK-TMR calculated from direct measurements and from the competitive binding protocol are based on paired sample t test, where the daily values were paired and compared. The same method was utilized to compare the reaction rate constants calculated from direct measurements for CHO-NLFNYK-FL and CHO-NLFNYK-TMR.

RESULTS

In this paper, we have validated the utility of competitive binding protocols for evaluating the kinetic binding dynamic of unlabeled ligands. Additionally, we calibrate the relative intensity of flow cytometric fluorescence measurements to numbers of bound ligands, including the potential quenching or enhancement of fluorescence caused by receptor-ligand interaction, for several new N-formyl peptide ligands.

Spectrofluorometric Determination of the Quantum Yield Ratio, F

The spectrofluorometric calibration method described by Fay et al. (4) was used to calibrate serial dilutions of the labeled ligands CHO-MLFK-FL, CHO-NLFFK-FL, N- CHO-MLFFK-FL, CHO-NLFNYK-FL, CHO-NLFNYK-Bodipy, and CHO-NLFNYK-TMR to standard free fluorescein solutions and to calculate F, the ratio of fluorescence of fluorescein to fluorescent ligand. The ratio of the emission readings of the fluorescently labeled ligand to the free fluorescein was calculated and resulted in the quantum yield ratio F, as summarized in Table 1.

Flow Cytometric Determination of the Calibration Number Q

Equilibrium binding studies were used to determine the value of the calibration number Q for the different ligands relative to CHO-NLFNYK-FL. Figure 2 depicts representative histograms of equilibrium binding data for fluorescently labeled ligands at an emission wavelength of 530 nm and 585 nm. Different concentration ranges were used for the various ligands based on their affinities for the N-formyl peptide receptor. Note that the fluorescein-labeled calibration beads had significant emission at 585 nm and therefore could be used to calculate the calibration number for CHO-NLFNYK-TMR. Furthermore, even though the excitation wavelength (488 nm) was not optimal for tetramethylrhodamine (see Fig. 1), the ligand emission was distinguishable from the cellular background fluorescence. Mean channel numbers for each histogram were calculated and equilibrium-binding curves (see Fig. 3) were obtained as described in Methods. The

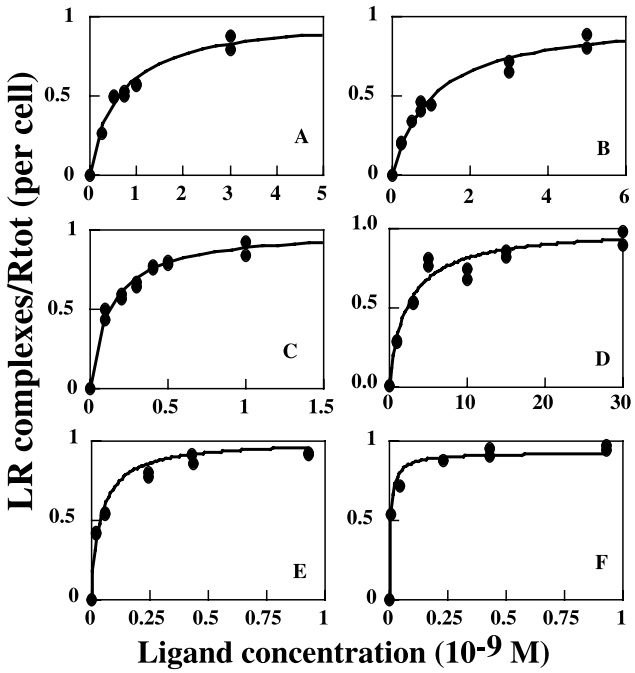

FIG. 3. Equilibrium binding curves. Representative equilibrium binding curves of receptor-ligand complexes normalized to the experimental R_{tot} versus the ligand concentration for CHO-NLFNYK-FL (**A**), CHO-NLFNYK-Bodipy (**B**), CHO-MLFK-FL (**C**), CHO-NLFNYK-TMR (**D**), CHO-NLFFK-FL (**E**), and CHO-MLFFK-FL (**F**). Data in panels A–D were collected on the same day for which R_{tot} (determined with CHO-NLFNYK-FL) was 39,892 receptors/cell. Data in panels E and F were collected on a different day with cells from a different donor; For this experiment R_{tot} (determined with CHO-NLFNYK-FL) was 44,606.

value Q was determined for test ligands relative to CHO-NLFNYK-FL with the assumption of constant R_{tot} as described in Methods. These calculated Q numbers are summarized in Table 1.

Evaluation of Quenching Ratio, I_b/I_f

Predicted values of I_b/I_f, the ratio of fluorescence intensity of bound to free ligand, were calculated from the Q values obtained flow cytometrically and the F values determined spectrofluorometrically (Table 1). For three of the ligands, the ratio I_b/I_f has been reported utilizing the antibody-quenching approach of Fay et al. (4), although the emission wavelength for their studies differed slightly from ours (520 nm versus 530 nm). Our predicted I_b/I_f ratios agree well with these previously published values. The fluorescence intensity ratios of bound versus free ligand could not be directly quantified for Bodipy and TMR labeled ligands because of a lack of antibodies that sufficiently quenched the fluorescence of these moieties. However, Figure 4 displays representative data qualitatively showing the quenching (or lack thereof) for these ligands for which I_b/I_f had not been previously reported. Our predicted I_b/I_f ratios were in good agreement with the qualitative measurements of quenching shown in Figure 4.

Equilibrium Binding Constants

The equilibrium binding experiments were also used to obtain the apparent equilibrium dissociation constants, K_{dapp}, for the ligands tested (Table 2). Although all of these peptide ligands bound to the same site on the N-formyl peptide receptor, there was a nearly two-order of magnitude range in the K_{dapp}, from 0.06 nM to 2.55 nM. Interestingly, the identity of the fluorescent tag influenced

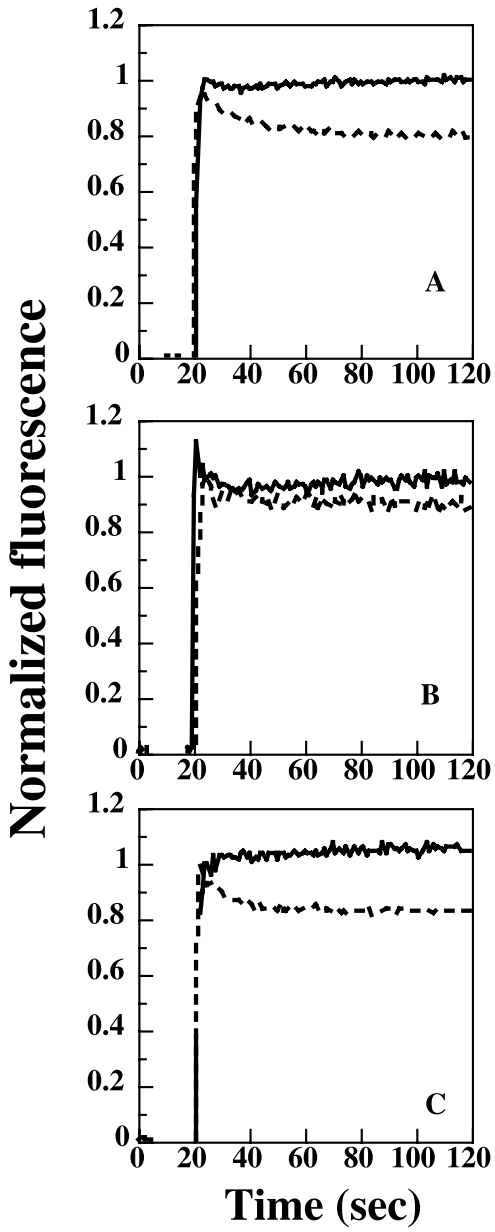

FIG. 4. Qualitative assessment of quenching of ligand fluorescence upon binding. Data was obtained spectrofluorometrically as described in Methods using a cell concentration of 1×10^7 cells/ml for CHO-NLFNYK-Bodipy (**A**), CHO-NLFNYK-TMR (**B**), and CHO-NLFFK-FL (**C**). Data was collected in the presence (solid traces) and absence (dashed traces) of a nonfluorescent receptor antagonist, t-Boc. Predicted values of normalized fluorescence caused by ligand quenching, calculated from K_{dapp} and predicted I_b/I_f with the assumption of 0.66 nM receptor concentration (i.e., 40,000 receptors/cell), were 0.92, 0.99, and 0.61, respectively.

Table 2
Equilibrium Dissociation Constants ($K_{d_{app}}$) at 4°C

Ligand	$K_{d_{app}}$ (nM)[a]	Reported $K_{d_{app}}$ (nM)
CHO-NLFNYK-FL	0.55 ± 0.04 (39)	0.35 ± 0.2[b]
CHO-NLFNYK-Bodipy	0.97 ± 0.18 (11)	
CHO-NLFNYK-TMR	2.55 ± 0.25 (30)	
CHO-MLFFK-FL	0.06 ± 0.02 (5)	0.03[c]
CHO-NLFFK-FL	0.07 ± 0.01 (5)	
CHO-MLFK-FL	0.12 ± 0.02 (10)	0.04[c]

[a]Mean ± SEM, *n* in parentheses.
[b]From Hoffman et al. in intact cells (8).
[c]From Fay et al. in permeabilized cells (24).

the binding of the ligand to the receptor as seen by the differences in K_{dapp} for the three ligands with the same peptide sequence (CHO-NLFNYK-FL, CHO-NLFNYK-Bodipy, and CHO-NLFNYK-TMR). The calculated K_{dapp} values correlate well with previously published values of equilibrium binding constants that are available for some of the ligands tested.

Ligand-Dependent Binding Rate Constants via Direct Binding Protocols

The binding and dissociation of two fluorescent ligands, CHO-NLFNYK-FL and CHO-NLFNYK-TMR, were monitored using flow cytometry (protocols A and B) with emission wavelengths of 530 nm and 585 nm, respectively. Data were fit to the two-site binding model to obtain values of the rate constants k_f, k_r, k_x, k_{f2}, and k_{r2}, constraining the ratio k_{r2}/k_{f2} to be equal to the value of K_{dapp} calculated from equilibrium binding experiments. Figure 5 depicts kinetic binding data collected via three different direct measurements for CHO-NLFNYK-TMR. The solid lines show the fit of the two site binding model to these data. The reaction rate constants describing binding, k_f, and dissociation, k_r, of the low-affinity receptor/ligand complex, and receptor affinity conversion, k_x, were calculated from association binding data and 90-s dissociation data, as significant numbers of the low-affinity receptor/ligand complex are present for these experimental time scales. The reaction rate constants governing the lifetime of the high-affinity state, k_{f2} and k_{r2}, were evaluated from long-time, or 2-h, dissociation data, as significant numbers of the high affinity receptor/ligand complex are present at this experimental time scale. The same type of data collection was carried on for CHO-NLFNYK-FL at a different emission wavelength, 530 nm, as has been previously reported (8). The values of the reaction rate constants calculated based on these direct measurements are listed in Table 3.

The ligands CHO-NLFNYK-FL and CHO-NLFNYK-TMR differ only in the fluorescent tag, and not in the peptide sequence. Using a paired sample *t* test to compare the values of the reaction rate constants calculated for each day and for each ligand, all the reaction rate constants can be shown to be statistically different except for the dissociation rate constant, k_r. Thus most of the reaction rate constants describing the two site binding model of the N-formyl peptide receptor are ligand dependent, even for these two very similar ligands. It is not clear from the present study whether the dissociation constant k_r is entirely ligand independent or simply more dependent upon the peptide sequence than the fluorescent tag, although an earlier study (22) using different ligands for the N-formyl peptide receptor shows k_r to be ligand dependent.

Ligand-Dependent Binding Rate Constants via Competitive Binding Protocols

The binding of unlabeled ligand is indirectly measured by the effect it has on the binding of the labeled ligand. The tetramethylrhodamine labeled ligand, CHO-NLFNYK-TMR, does not have significant emission at the lower

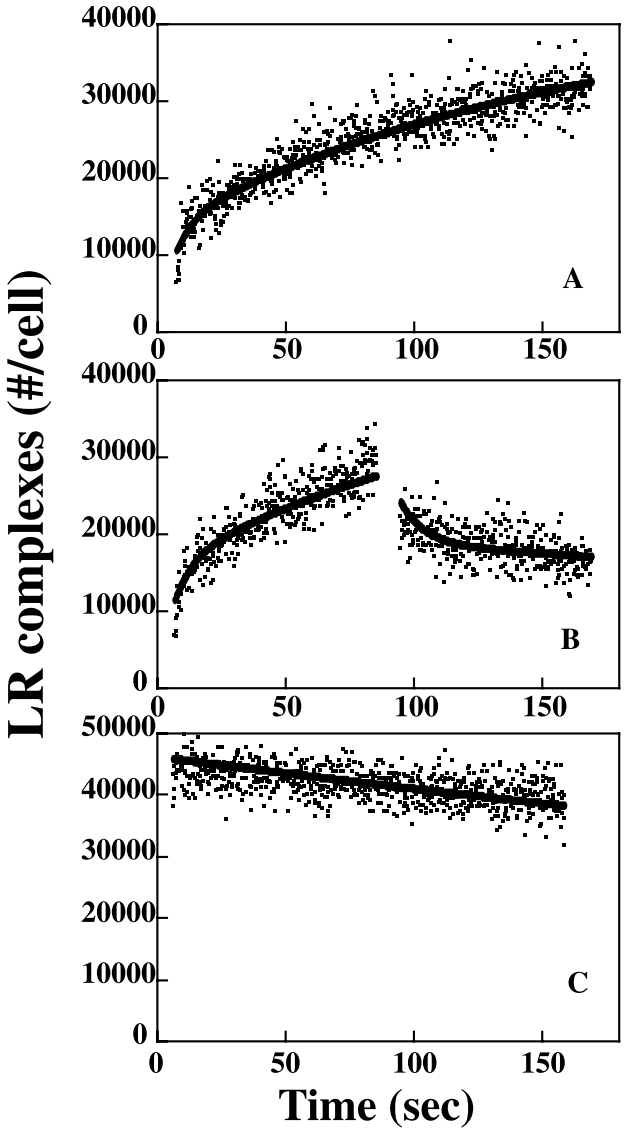

FIG. 5. Direct measurements of CHO-NLFNYK-TMR binding. Kinetic binding data (dots) and model fit (line) for CHO-NLFNTNK-TMR binding to the N-formyl peptide receptor collected via association protocol (**A**), 90-s dissociation protocol (**B**), and 2-h dissociation protocol (**C**) at 585 nm. These data were all taken on the same day (single donor).

Table 3
Reaction Rate Constants for CHO-NLFNYK-FL and CHO-NLFNYK-TMR

Rate constants	CHO-NLFNYK-FL direct measurement[d]	CHO-NLFNYK-TMR direct measurements[d]	CHO-NLFNYK-TMR competitive binding[d]
k_f (M^{-1} s^{-1})[a]	$7.4 \pm 0.5 \times 10^6$ (16)[e]	$3.1 \pm 0.2 \times 10^6$ (16)	$3.37 \pm 0.3 \times 10^6$ (7)[f]
k_r (s^{-1})[a]	$1.14 \pm 0.06 \times 10^{-1}$ (16)	$1.23 \pm 0.05 \times 10^{-1}$ (16)	$1.40 \pm 0.2 \times 10^{-1}$ (7)[f]
k_x (s^{-1})[b]	$2.36 \pm 0.1 \times 10^{-2}$ (16)[e]	$1.45 \pm 0.09 \times 10^{-2}$ (16)	$1.91 \pm 0.07 \times 10^{-2}$ (7)[f]
k_{r2} (s^{-1})[c]	$9.33 \pm 1.0 \times 10^{-4}$ (16)[e]	$1.31 \pm 0.08 \times 10^{-3}$ (16)	$0.31 \pm 0.07 \times 10^{-3}$ (4)
k_{f2} (M^{-1} s^{-1})[c]	$2.10 \pm 0.2 \times 10^6$ (16)[e]	$6.17 \pm 0.5 \times 10^5$ (16)	$0.89 \pm 4 \times 10^5$ (4)

[a]Binding rate constants calculated from association and 90-s dissociation protocols for direct methods and from competitive association protocol.
[b]Binding rate constants calculated from direct association and 90-s dissociation protocol or short-time displacement protocol for competitive binding.
[c]Binding rate constants evaluated with the constraint on k_{f2} from equilibrium binding constraint, $K_{d\text{app}} = k_{r2}/k_{f2}$, from 2-h dissociation for direct measurements or from long-time displacement protocols for competitive binding.
[d]Mean ± SEM, n in parentheses.
[e]Statistically different from values determined by direct measurements for CHO-NLFNYK-TMR.
[f]Statistically the same as the values determined by direct measurements for CHO-NLFNYK-TMR.

emission wavelength (530 nm) when excited at 488 nm; it can be used as an unlabeled ligand when observing fluorescent at the FL1 channel. Different concentration ratios were tested given the constraints listed in Methods, and the ratio of 6 nM/15 nM of CHO-NLFNYK-FL versus CHO-NLFNYK-TMR yielded optimal results.

Competitive association binding of CHO-NLFNYK-FL and CHO-NLFNYK-TMR (protocol C) is shown in Figure 6. For comparison, binding of CHO-NLFNYK-FL alone is also shown. When CHO-NLFNYK-FL fluorescence is monitored in the presence of unlabeled ligand (CHO-NLFNYK-TMR), less binding occurs than for CHO-NLFNYK-FL alone, consistent with competition of the two ligands for the receptor. This difference in binding was used to calculate the reaction rate constants governing the formation of the low-affinity receptor-ligand complex for the unlabeled ligand CHO-NLFNYK-TMR.

Displacement of unlabeled ligand by the labeled ligand (protocol D) was monitored at different timescales to capture the different dynamic states of the receptor. Short-time displacement data (Fig. 7A) were collected with the same ratio of ligand concentrations as in the

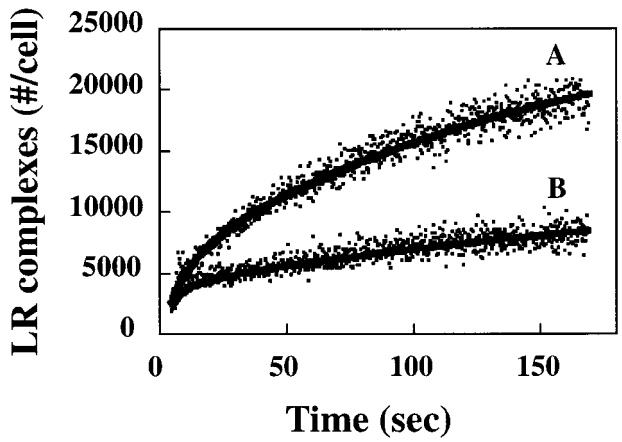

FIG. 6. Competitive association binding. Kinetic binding data (dots) and model fits of association kinetic binding of 6 nM CHO-NLFNYK-FL (trace **A**) and competitive association binding of a mixture of 6 nM CHO-NLFNYK-FL and 15 nM CHO-NLFNYK-TMR (trace **B**) measured at an emission wavelength of 530 nm.

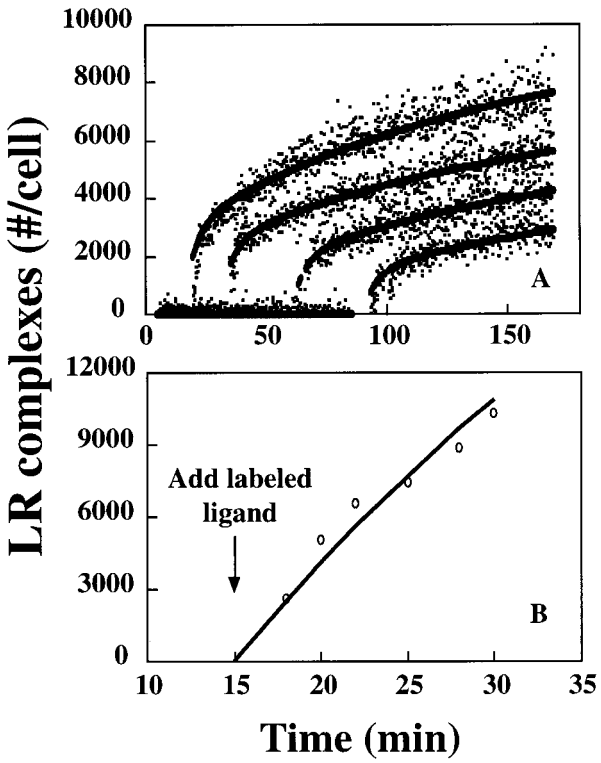

FIG. 7. Displacement data at variable timescales. Data of prebound CHO-NLFNYK-TMR being displaced by CHO-NLFNYK-FL (dots) collected at 530 nm under various timescales; short-timescale (**A**) where 15 nM of CHO-NLFNYK-TMR was incubated with cells at 10^6/ml for 15, 30, 60, or 90 s prior to the addition of 6 nM CHO-NLFNYK-FL and long-timescales (**B**) where 30 nM of CHO-NLFNYK-TMR was incubated with cells for at least 15 min prior to the addition of 250 nM of CHO-NLFNYK-FL. The short-time displacement data were fit with a two-site binding model (line), and the long-time displacement data were fit with single-site binding model (line) describing the high-affinity state of the N-formyl peptide receptor.

competitive association data. The unlabeled ligand CHO-NLFNYK-TMR was allowed to bind for 15 s or up to 90 s before addition of the labeled ligand CHO-NLFNYK-FL. The initial receptor-ligand complex had a low affinity for ligand and the dynamic existence of this low-affinity receptor state was evident in the short-time displacement data. At earlier time points (i.e., 15 s), the labeled ligand rapidly displaced the unlabeled ligand from the low-affinity receptor, while at later time points (i.e., 90 s) more of the receptors had converted into the high-affinity state and the displacement of the unlabeled ligand was slower.

The long-time displacement data, shown in Figure 7B, resulted in estimates for the dissociation reaction rate constant from the high-affinity receptor state, k_{r2}. This method required extensive optimizations regarding the ligand concentrations to utilize and when to initiate the displacement, as described in Methods. The concentrations of 30 nM CHO-NLFNYK-TMR and 250 nM of CHO-NLFNYK-FL were utilized and the nonspecific binding was blocked with 0.1 mM CHO-MLF. Furthermore, from the estimates of the binding rate constants we verified that 30 nM CHO-NLFNYK-TMR binding for 15 min resulted in over 90% conversion of the surface receptors to the high-affinity state.

The reaction rate constants for CHO-NLFNYK-TMR calculated from the competitive binding protocols are listed in Table 3. Statistically, the binding rate constants describing the formation and lifetime of the low-affinity receptor state, k_f, k_r, and k_x, as calculated from competitive binding protocols, were no different from the reaction rate constants calculated from direct measurements, according to a paired sample *t*-test analysis. However, reaction rate constants describing the high-affinity receptor state, k_{r2} and k_{f2}, were not statistically similar. These reaction rate values were less than an order of magnitude different from the values determined from direct binding measurements. Thus we conclude that the competitive binding protocol provided estimates of k_f, k_r, and k_x that were identical to those measured directly, and provided estimates of k_{r2} and k_{f2} that were accurate to within an order of magnitude.

DISCUSSION

In this paper, we have extended the methods of Fay et al. (4) for calibrating flow cytometric mean channel numbers to number of bound ligands to include the calibration of ligands labeled with fluorophores other than fluorescein. The calibration parameter, Q, represents the number of bound ligands per fluorescein equivalent and together with fluorescein-labeled standardized beads allows conversion of the relative flow cytometric intensity measurements to bound ligand per cell. These calibration values are essential for quantifying receptor-ligand interactions and obtaining rate constants for receptor-ligand binding. We utilized these values when evaluating the kinetic binding dynamics of two different fluorescently labeled ligands for validating competitive binding protocols.

The calibration strategy employed was to establish a calibration value by spectrofluorometric measurements for one fluorescent ligand compared to a standard bead fluorescence (fluorescein in this study). The calibration parameters, Q, for the other ligands were easily calculated based on flow cytometric equilibrium binding data. This approach is generally applicable to other cell surface receptor systems with the restriction that all the fluorescently labeled ligands bind to the same receptor site with known stoichiometry (one ligand to one receptor, in this case).

The calibration studies also yielded equilibrium dissociation constants for a set of six ligands, all of which bind to the N-formyl peptide receptor. Interestingly, these affinities varied significantly for these peptides, and even varied between identical peptides (NLFNYK) with different fluorescent tags (FL, Bodipy, TMR). Sklar et al. (20) have reported that the fluorescein on CHO-NLFNYK-FL is not in the binding pocket of the N-formyl peptide receptor, and hence it was an unexpected result that the fluorescent tag, which is outside of the binding pocket, would still influence the binding. This observation suggests that the fluorescent moiety interacts with the receptor on regions outside of the binding pocket.

Additionally, we have validated a set of competitive binding protocols applicable for analyzing receptor-ligand interactions described by a two site binding model. The competitive binding protocols described yielded statistically similar reaction rate constants to those calculated from direct measurements for the formation and lifetime of the low-affinity receptor state (k_f, k_r, and k_x). Because the low-affinity form of the receptor is thought to be the signaling state (22,23), the values of these rate constants are most important and can be used to understand the role that binding dynamics plays in cell activation. These competitive binding protocols were able to estimate reaction rate constants regulating the high-affinity receptor state (k_{r2} and k_{f2}) within an order of magnitude. The use of competitive binding protocols will greatly expand the number of ligands, including unlabeled and low-affinity ligands, available for future quantitative studies.

Finally, although the studies presented here focused on the neutrophil, these calibration methods and kinetic binding measurement techniques are applicable to other cellular receptor systems. We also speculate that our finding of ligand-dependent receptor binding and processing rate constants will be shown to be true for many other receptor systems.

ACKNOWLEDGMENTS

We thank Megan Taack for help with initial data analysis.

LITERATURE CITED

1. Linderman JJ. Kinetic modeling approaches to understanding ligand efficacy. In: Kenakin T, Angus JA, Black JW, Barr AJ, editors. The pharmacology of functional, biochemical, and recombinant receptor systems. Handbook of experimental pharmacology. New York: Springer-Verlag; 2000. p 119–146.
2. Lauffenburger DA, Linderman JJ. Receptors: models for binding, trafficking, and signaling. New York: Oxford University Press; 1993. 365 p.
3. Sklar LA, Jesaitis AJ, Painter RG, Cochrane CG. Ligand/receptor internalization: a spectroscopic analysis and a comparison of ligand binding, cellular response, and internalization by human neutrophils. J Cell Biochem 1982;20:193–202.
4. Fay SP, Posner RG, Swann WN, Sklar LA. Real-time analysis of the

assembly of ligand, receptor, and G-protein by quantitative fluorescence flow cytometry. Biochem 1991;30:5066–5075.
5. Murphy RF. Ligand binding, endocytosis, and processing. In: Melamed MR, Lind T, Mendelsohn ML, editors. Flow cytometry and sorting. 2nd ed. New York: Wiley-Liss; 1990. p 355–366.
6. Kenakin T. Pharmacologic analysis of drug-receptor interaction. New York: Raven; 1993. 483 p.
7. Sklar LA, Sayre J, McNeil VM, Finney DA. Competitive binding kinetics in ligand-receptor-competitor systems: rate parameters for unlabeled ligands for the formyl peptide receptor. Mol Pharmacol 1985; 28:323–330.
8. Hoffman JF, Keil ML, Riccobene TA, Omann GM, Linderman JJ. Interconverting receptor states at 4 degrees C for the neutrophil N-formyl peptide receptor. Biochemistry 1996;35:13047–13055.
9. Vilven JC, Domalewski M, Prossnitz ER, Ye RD, Muthukumaraswamy N, Harris RB, Freer RJ, Sklar LA. Strategies for positioning fluorescent probes and crosslinkers on formyl peptide ligands. J Recept Signal Transduct Res 1998;18:187–221.
10. Freer RJ, Day AR, Muthukumaraswamy N, Pinon D, Wu A, Showell HJ, Becker EL. Formyl peptide chemoattractants: a model of the receptor on rabbit neutrophils. Biochemistry 1982;21:257–263.
11. Rot A, Henderson LE, Copeland TD, Leonard EJ. A series of six ligands for the human formyl peptide receptor: tetrapeptides with high chemotactic potency and efficacy. Proc Natl Acad Sci U S A 1987;84: 7967–7971.
12. Sklar LA. Real-time spectroscopic analysis of ligand-receptor dynamics. Annu Rev Biophys Biophys Chem 1987;16:479–506.
13. Sklar LA, Mueller H, Omann GM, Oades ZG. Three states for the formyl peptide receptor on intact cells. J Biol Chem 1989;264:8483–8486.
14. Sklar LA, Oades ZG, Jesaitis AJ, Painter RG, Cochrane CG. Fluoresceinated chemotactic peptide and high-affinity antifluorescein antibody as a probe of the temporal characteristics of neutrophil stimulation. Proc Natl Acad Sci U S A 1981;78:7540–7544.
15. Niedel JE, Kahane I, Cautrecases P. Receptor mediated internalization of fluorescent chemotactic peptide by human neutrophils. Science 1979;205:1412–1414.
16. Mercola DA, Morris JW, Arquilla ER. Use of resonance interaction in the study of the chain folding of insulin in solution. Biochemistry 1972;11:3860–3874.
17. Sklar LA, Oades ZG, Finney DA. Neutrophil degranulation detected by right angle light scattering: spectroscopic methods suitable for simultaneous analyses of degranulation or shape change, elastase release, and cell aggregation. J Immunol 1984;133:1483–1487.
18. Tolley JO, Omann GM, Jesaitis AJ. A high yield, high-purity elutriation method for preparing human granulocytes demonstrating enhanced experimental lifetimes. J Leuk Biol 1987;42:43–50.
19. Nash TJ. Interactions of un-ionized fluorescein. I. Color discharge by solvents and colloids. J Phys Chem 1958;62:1574–1578.
20. Sklar LA, Fay SP, Seligmann BE, Freer RJ, Muthukumaraswamy N, Mueller H. Fluorescence analysis of the size of a binding pocket of a peptide receptor at natural abundance. Biochemistry 1990;29:313–316.
21. Sklar LA, Finney DA. Analysis of ligand-receptor interactions with the fluorescence activated cell sorter. Cytometry 1982;3:161–165.
22. Hoffman JF, Linderman JJ, Omann GM. Receptor up-regulation, internalization, and interconverting receptor states. Critical components of a quantitative description of N-formyl peptide-receptor dynamics in the neutrophil. J Biol Chem 1996;271:18394–18404.
23. Sklar LA, Finney DA, Oades ZG, Jesaitis AJ, Painter RG, Cochrane CG. The dynamics of ligand-receptor interactions. Real-time analyses of association, dissociation, and internalization of an N-formyl peptide and its receptors on the human neutrophil. J Biol Chem 1984;259: 5661–5669.
24. Fay SP, Domalewski MD, Sklar LA. Evidence for protonation in the human neutrophil formyl peptide receptor binding pocket. Biochemistry 1993;32:1627–1631.

APPENDIX

Model I describes the binding of a fluorescently labeled ligand L. The binding of an unlabeled ligand U is described by:

$$U + R_s \underset{k_{ru}}{\overset{k_{fu}}{\rightleftharpoons}} UR_s \overset{k_{xu}}{\longrightarrow} UR_x \underset{k_{f2u}}{\overset{k_{r2u}}{\rightleftharpoons}} U + R_x \quad \text{(Model AI)}$$

The apparent receptor-ligand complex number that is measured by flow cytometry, [LR]app, is equal to:

$$[LR]_{\text{app}} = [LR_s] + [LR_x] \tag{A1}$$

The differential equations describing Models I and AI are listed below. For analysis of only labeled ligand binding, the concentration of the unlabeled ligand, [U], is equal to zero.

$$d[LR_s]/dt = k_f[L][R_s] - (k_r + k_x)[LR_s] \tag{A2}$$

$$d[LR_x]/dt = k_x[LR_s] - k_{r2}[LR_x] + k_f[L][R_x] \tag{A3}$$

$$d[UR_s]/dt = k_{fu}[U][R_s] - (k_{ru} + k_{xu})[UR_s] \tag{A4}$$

$$d[UR_x]/dt = k_{xu}[UR_s] - k_{r2u}[UR_x] + k_{fu}[U][R_x] \tag{A5}$$

$$d[R_x]/dt = k_{r2}[LR_x] - k_{f2}[L][R_x] + k_{r2u}[UR_x] + k_{f2u}[U][R_x] \tag{A6}$$

$$d[R_s]/dt = k_r[LR_s] - k_f[L][R_s] - k_{fu}[U][R_s] + k_{ru}[UR_s] \tag{A7}$$

$$d[L]/dt = \{-k_f[L][R_s] + k_r[LR_s] + k_{r2}[LR_x] - k_{f2}[L][R_x]\} \times \{n(Av)^{-1}(V)^{-1}\} \tag{A8}$$

$$d[U]/dt = \{-k_{fu}[U][R_s] + k_{ru}[UR_s] + k_{r2u}[UR_x] - k_{f2u}[U][R_x]\}\{n(Av)^{-1}(V)^{-1}\} \tag{A9}$$

V is the assay volume in liters, n is the number of cells in the assay volume, and Av is Avogadro's number.